Development of laser wakefield acceleration driven by few-TW pulses in a sub-mm, dense nitrogen gas target

Ming-Wei Lin[1,2*], Po-Wei Lai[1], and Dang Khoa Tran[1],
[1]*Institute of Nuclear Engineering and Science, National Tsing Hua University, Taiwan*

Shao-Wei Chou[2,3], Hsu-Hsin Chu[2,3], Shih-Hung Chen[2], and Jyhpyng Wang[2,3,4]
[2]*Department of Physics, National Central University, Taiwan*
[3]*Center for High Energy and High Field Physics, National Central University, Taiwan*
[4]*Institute of Atomic and Molecular Science, Academia Sinica, Taiwan*

Asian Forum for Accelerators and Detectors
April 12th, 2023

Criteria for operating laser wakefield acceleration (LWFA) in blowout regime

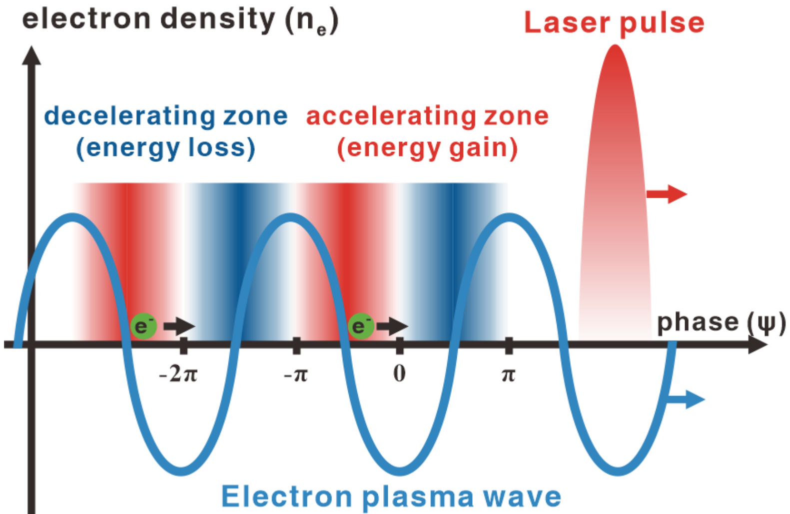

laser peak power

$$P_L = \sqrt{\frac{2}{\pi}\frac{E_p}{\tau_p}}$$

laser peak intensity

$$I_L = \frac{2}{\pi}\frac{P_L}{w_0^2}$$

normalized vector potential

$$a_0 = [7.3 * 10^{-19}\, I_L(W/cm^2)]^{1/2}\lambda_L(\mu m)$$

$a_0 > 1$ is desired to effectively excite nonlinear plasma waves

Critical power to reach the blowout regime

$$P^{cr}_{bubble} \sim \left(\frac{\tau_L[fs]}{\lambda_L[\mu m]}\right)^2 \times 30\ [GW]$$

τ = 40 fs, λ = 800 nm, f ≤10 Hz

P^{cr}_{bubble} ~ 75 TW

τ = 10 fs => P^{cr}_{bubble} ~ 4.7 TW

B. Hidding et al., Phys. Plasmas 16, 043105 (2009)

Conditions for the matched spot size and pulse duration in blow-out regime

$$k_p R \cong k_p w = 2\sqrt{a_0} \quad \textbf{or} \quad a_0 \cong 2\left(\frac{P_L}{P_{cr}}\right)^{1/3}$$

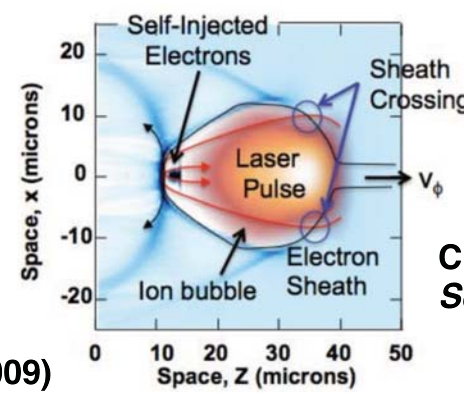

$$2c\tau_L \sim 2w \sim \lambda_p$$

C. Joshi , *IEEE Trans. Plasma Sci.* 45, 3134 (2017)

Self-focusing effect and self-modulation instabilities can greatly enhance the intensity of a few-/sub-TW pulse for driving LWFA

self-focusing effect

self-focusing critical power

$$P_{cr} \approx 17.4 \left(\frac{\omega_L^2}{\omega_p^2}\right) \mathrm{GW}$$

$$P_L > P_{cr}$$

transverse size reduction

$$2w \sim \lambda_P$$

ponderomotive self-focusing

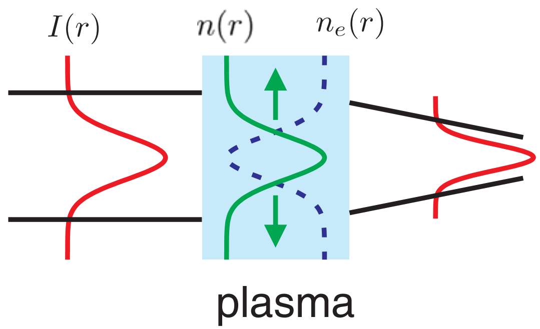

relativistic self-focusing

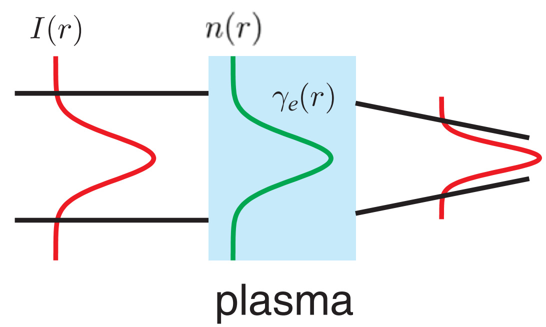

plasma frequency

$$\omega_p^2(r) = \frac{q_e^2 n_e(r)}{\epsilon_0 m_e \gamma_e(r)}$$

index of refraction

$$n(r) = \sqrt{1 - \frac{{\omega_p}^2(r)}{{\omega_L}^2}}$$

self-modulation instability

formation and longitudinal compression of micropulses

$$2c\tau_L \sim \lambda_P$$

incident pulse envelope

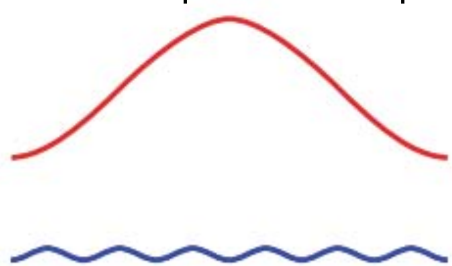

plasma density perturbation

modulated pulse envelope

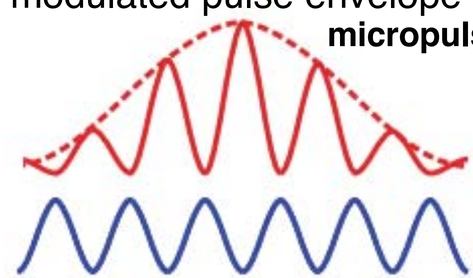

plasma wave

For 800-nm pulse :

n_e **~ 3 × 10^{19} cm^{-3} => P$_{cr}$ ~ 1 TW**

$\lambda_P \sim 2w \sim$ **6 µm** $\quad \tau_L$ **~ 10 fs**

Sub-TW LWFA can be achieved with the use of a thin, high-density gas target

Central to this approach is a thin, high density pulsed hydrogen gas jet produced by a 100-μm diameter needle orifice.

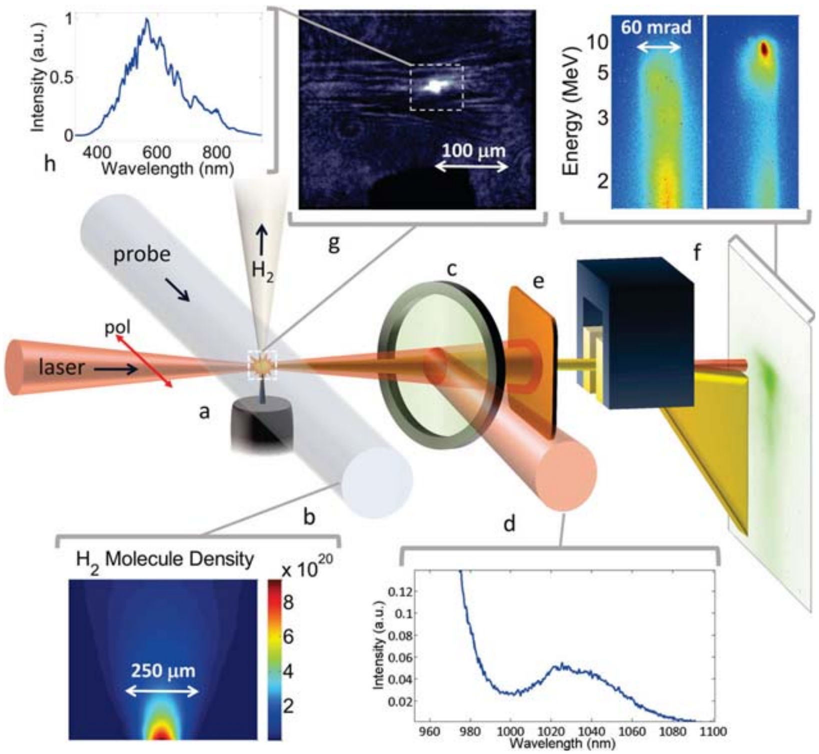

A. J. Goers, et al., Phys. Rev. Lett. 115, 194802 (2015)

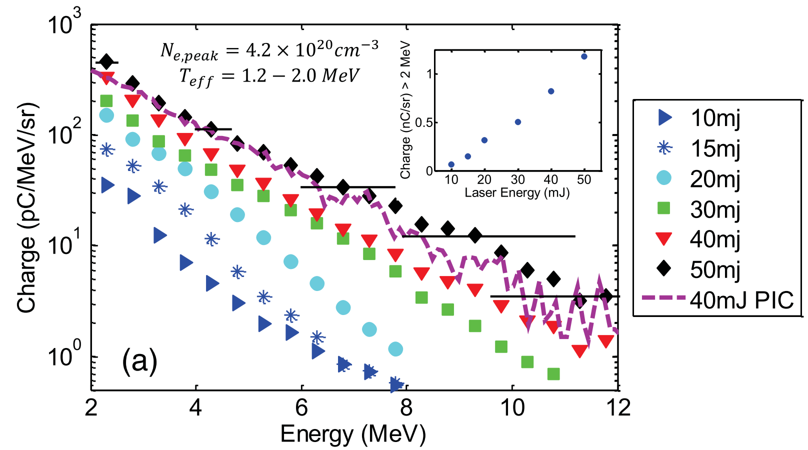

- **Introduce 50-fs, 800-nm pulses with an energy < 50 mJ into dense hydrogen gas jets with $n_{ep} > 10^{20}$ cm^{-3}.**
- **The thin (FWHM length ~ 250 μm), high-density hydrogen gas jet can reach a maximum peak molecular density of 9×10^{20} cm^{-3} with cryogenic cooling.**

MJ-level, few-cycle pulse are applied to drive sub-TW LWFA at a kHz-class frequency

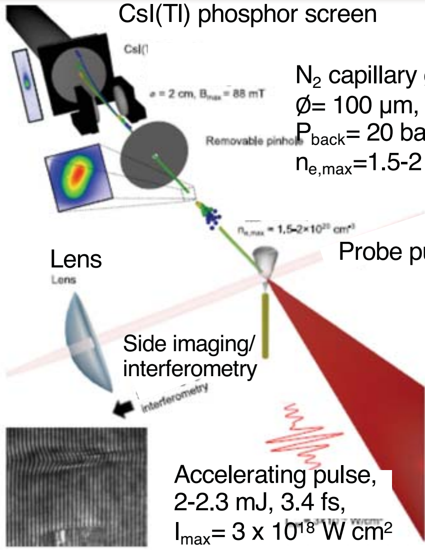

D. Guénot., et al, Nat. Photonics 11, 293 (2017).

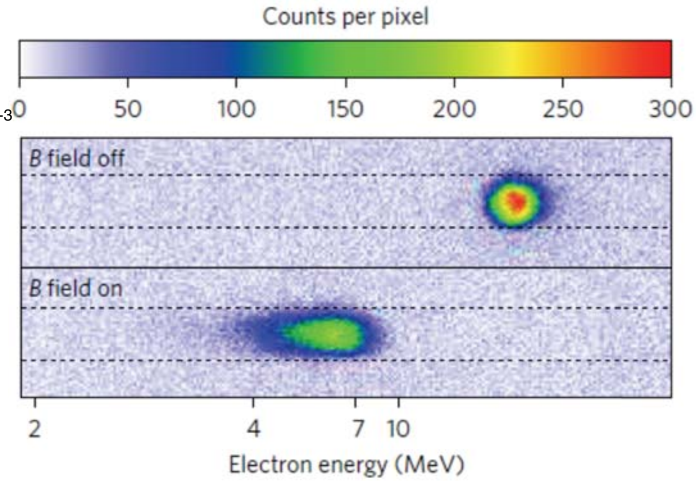

driving pulse:
2.1 mJ, 3.4 fs, 1 kHz

nitrogen target:
n_e=1.8 x 10^{20} cm^{-3}
Gaussian FWHM ~ 100 µm

output electrons:
E= 10 MeV
Q= 147 fC

driving pulse:
2.6 mJ, 5 fs, 1 kHz

hydrogen target:
n_e=2.2 x 10^{20} cm^{-3}
Gaussian FWHM ~ 150 µm

output electrons:
E= 15 MeV
Q= 2.5 pC

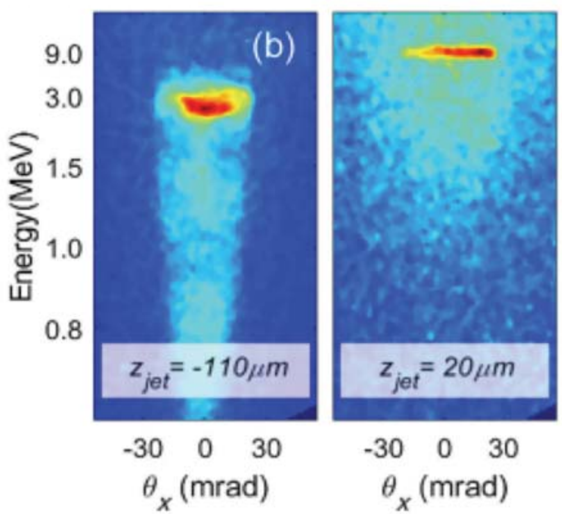

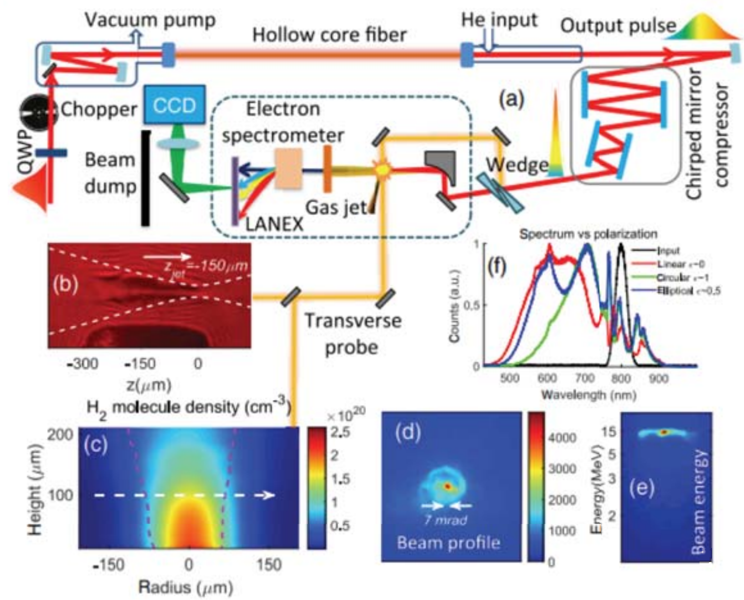

F. Salehi et al., Phys. Rev. X 11, 021055 (2021).

Few-TW LWFA vs. sub-TW LWFA for achieving high repetition-rate operation

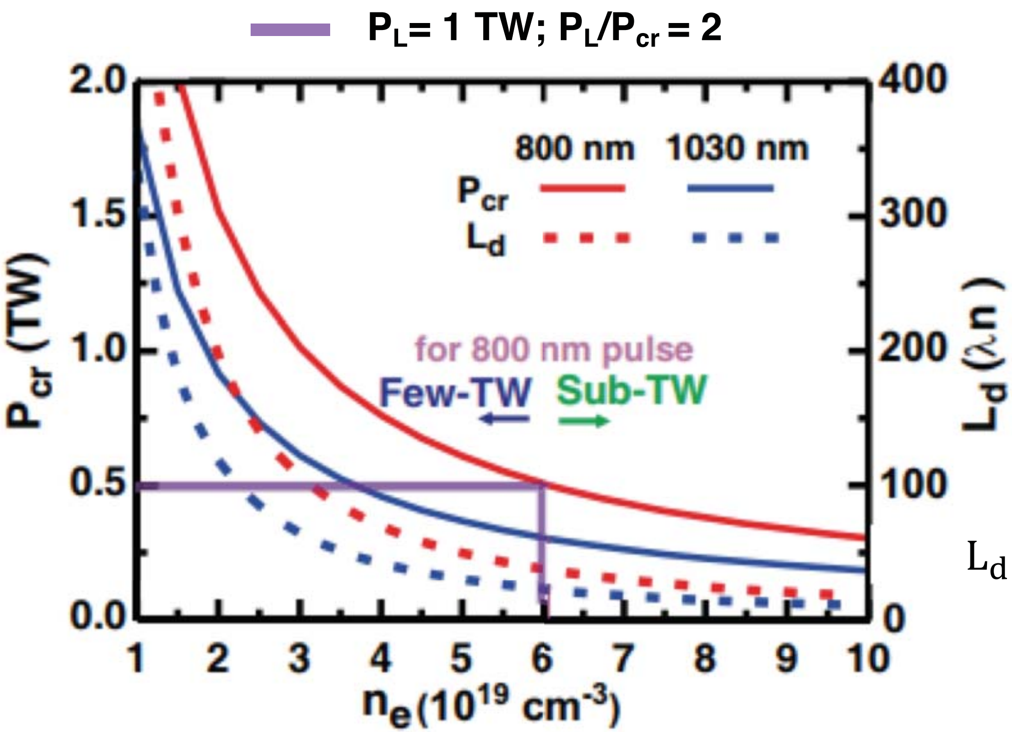

plasma wavelength

$$\lambda_p \approx \frac{2\pi}{\omega_p} \Rightarrow \lambda_p \propto n_e^{-1/2}$$

dephasing length

$$L_d \approx \frac{4}{3}\frac{c_0\omega_L^2}{\omega_p^3}\sqrt{a_0} \Rightarrow L_d \propto n_e^{-3/2}$$

Few-TW LWFA: Challenging for developing high-average-power, TW-level lasers

Sub-TW LWFA : Challenging for developing a thin, dense target

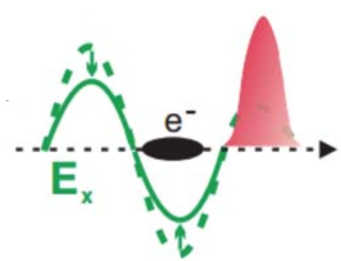

- **A short dephasing length and a low energy gain**
- **Beam loading can be significant at a pC-level bunch charge**

Novel kHz-class, TW-level pulse can be produced with related spectral broadening technique and applied to realize high-repetition-rate LWFA

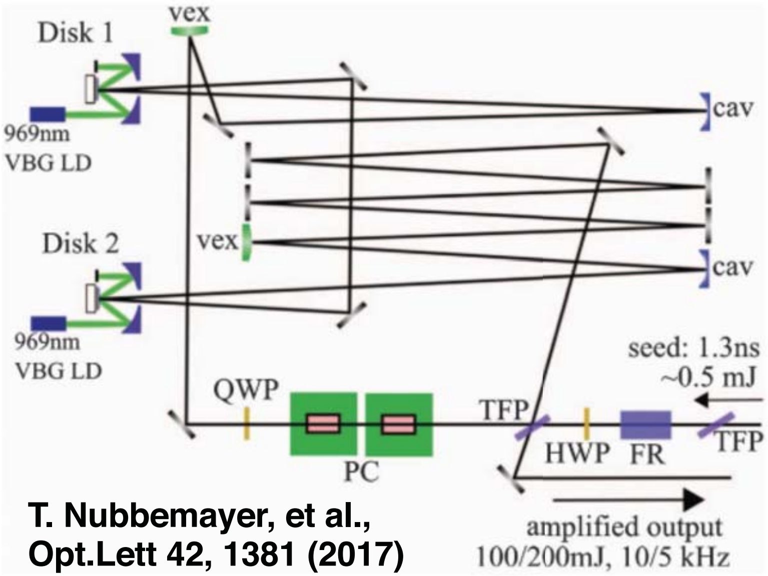

T. Nubbemayer, et al., Opt.Lett 42, 1381 (2017)

Regenerative amplifier

- Yb-YAG thin disk crystal, water cooled
- Pump source:
  CW mode of 969 nm diode laser with 3.5 kW
- Output pulse:
  1030 nm, 200 mJ, 1 ps@ 5 kHz

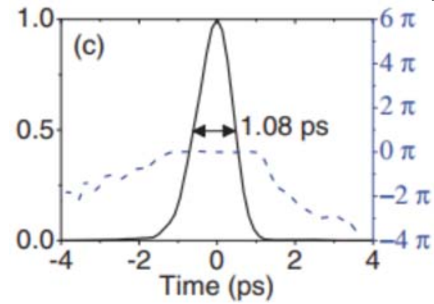

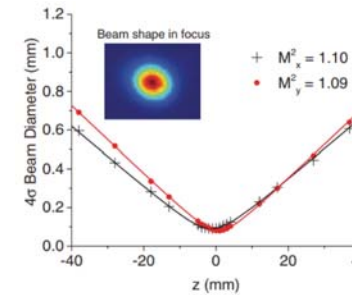

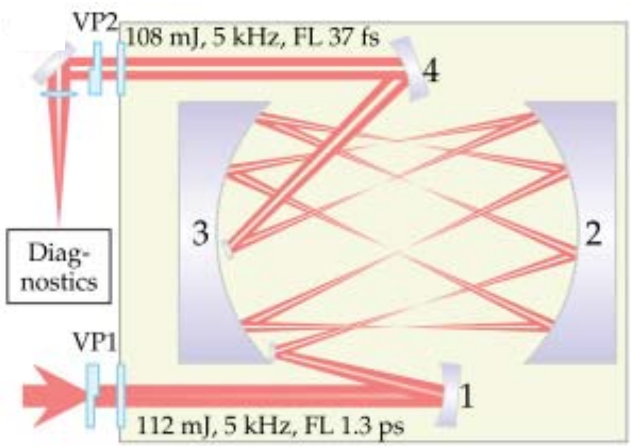

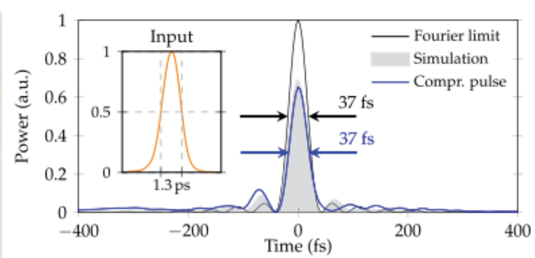

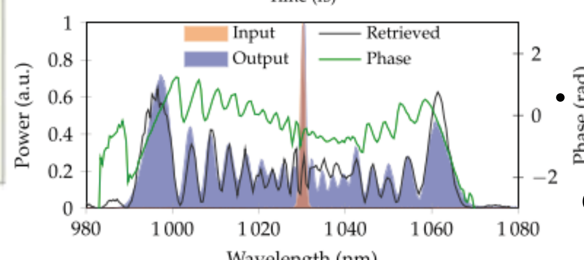

M. Kaussman, et al., Opt. Lett 46, 929 (2021)

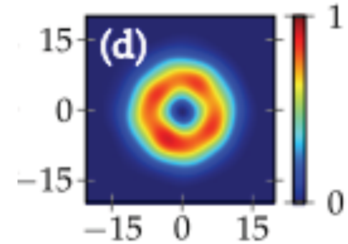

LG_{10} donut mode

Multipass cell

- Output:
  112 mJ, 37 fs @5 kHz
  conversion efficiency: 98 %

Our approach for developing few-TW LWFA with multi-cycle pulses rests upon the creation of sub-mm gas jets and gas cells

Investigate the sub-TW LWFA when the gas target exhibits a Gaussian density profile (gas jet) or a flat-top density distribution (gas cell).

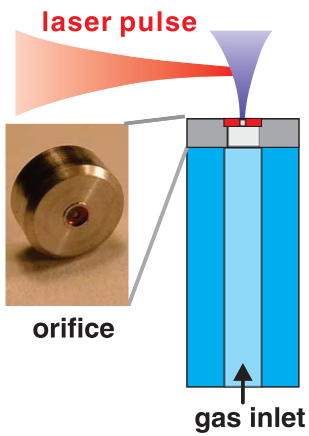

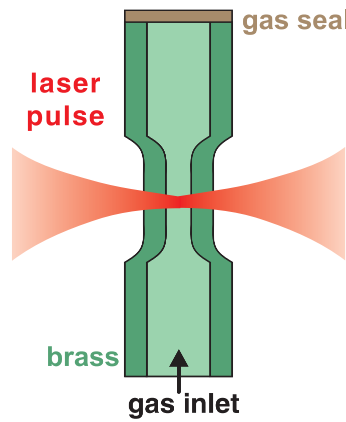

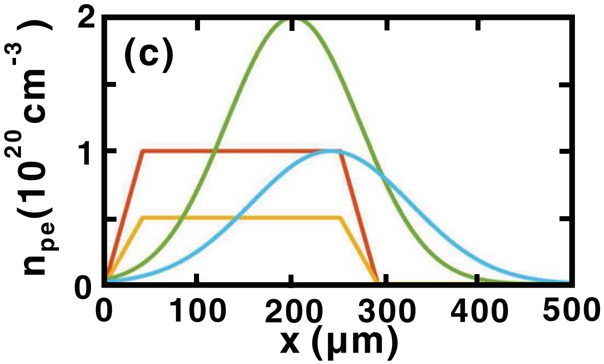

Simulation

- Particle-in-cell (PIC) simulation for few- / sub-TW LWFA
- Computational fluid dynamics(CFD) simulation for high-density gas cell and gas jet

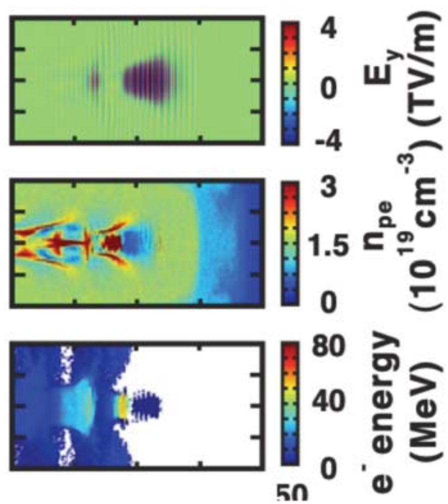

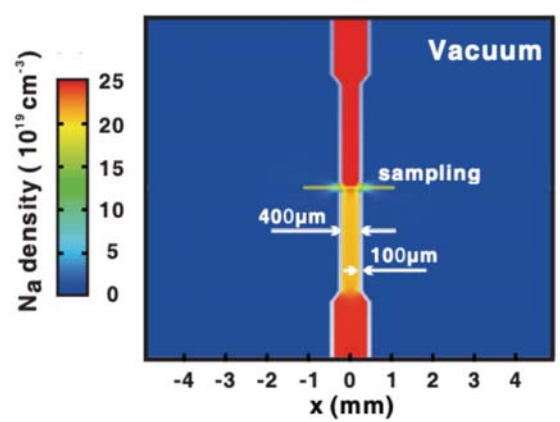

An experimental station for conducting LWFA driven by few-TW or sub-TW pulses is developed at NCU

Pump pulse: 40 fs, 800 nm, E_p -> 200 mJ

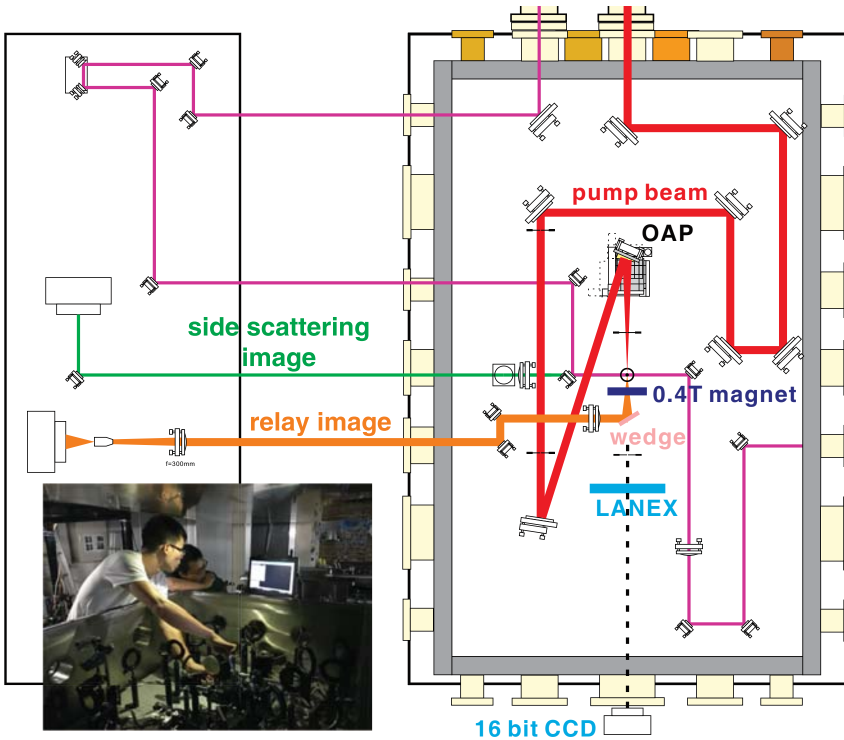

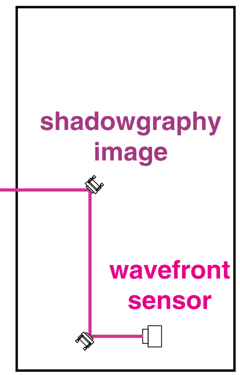

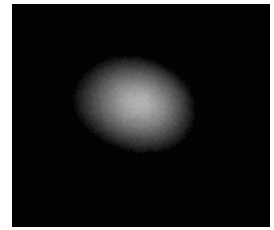

Off-axis parabolic mirror (OAP) : *f*/7

Spot size (FWHM):
vertical ~ 7.5 μm
horizontal ~ 12 μm
80 % energy enclosed in the Gaussian-fit profile

On target:
Peak power ~ 3.7 TW
Peak intensity ~ 3.3 x 10^{18} W/cm^2
a_0 ~ 1.2

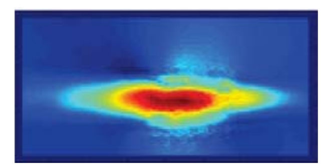

- **Electrons produced from LWFA is measured by a Kodak LANEX placed ~1.6 cm downstream the gas nozzle.**
- **With a 0.4-T magnet, energy spectrum 3 - 40 MeV can be resolved.**

- **Plasma density is measured by the probe pulse that passes the target and is recorded as the shadowgraphic image by the wavefront sensor.**

Thin, high-density gas target can be produced as the gas flow out from a nozzle having a diameter ~ 152 μm

Bird Precision

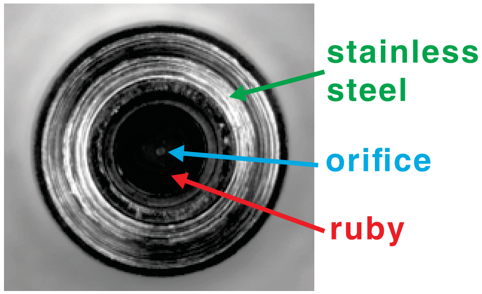

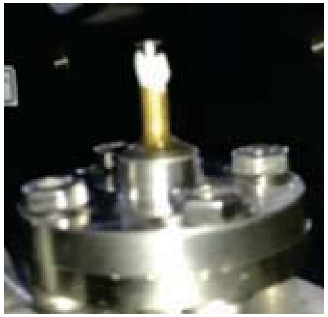

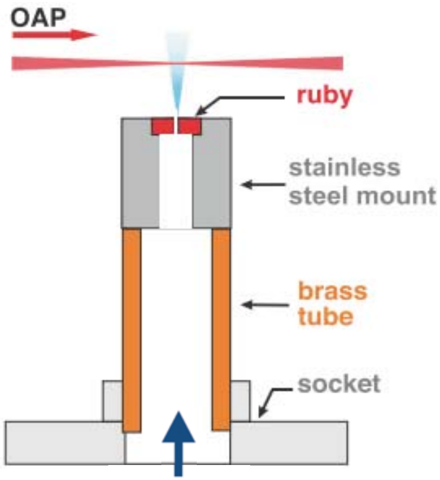

- The gas valve opens ~ 10 ms before the pump pulse enters the target region and lasts with a time interval of 5 ms.
- Density of the gas atoms/plasma in the target region can be varied by tuning the backing pressure of the gas supplied.

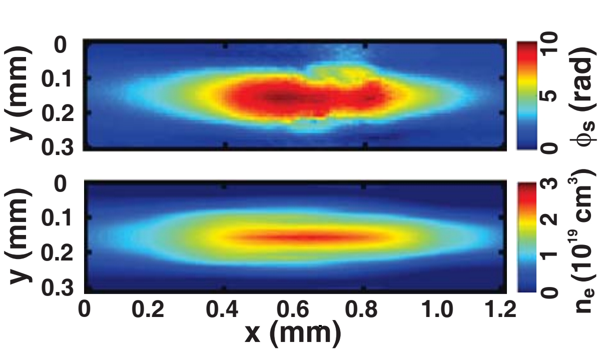

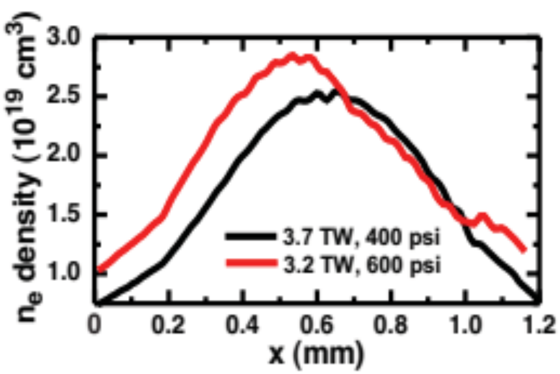

~ 860-μm (FWHM)
N plasma distribution

p_N = 400 psi
$n_{ep} \sim 2.5 \times 10^{19}$ cm^{-3}
p_N = 600 psi
$n_{ep} \sim 2.8 \times 10^{19}$ cm^{-3}

With P_L/P_{crp} ~ 3, electrons with peaks in 10 – 20 MeV can be routinely generated by 3.7-TW and 3.2 TW pulse

M.-W. Lin et al., Phys. Plasma 27, 103112 (2020).

Case I
3.7 TW, 400 psi
θy ~ 8.5 mad
θz ~ 22.5 mrad

Case III
3.2 TW, 600 psi
θy ~ 10.4 mad
θz ~ 23.6 mrad

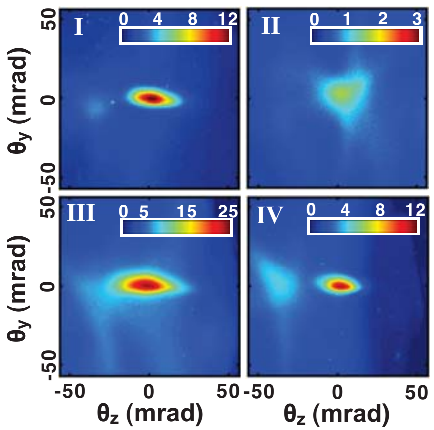

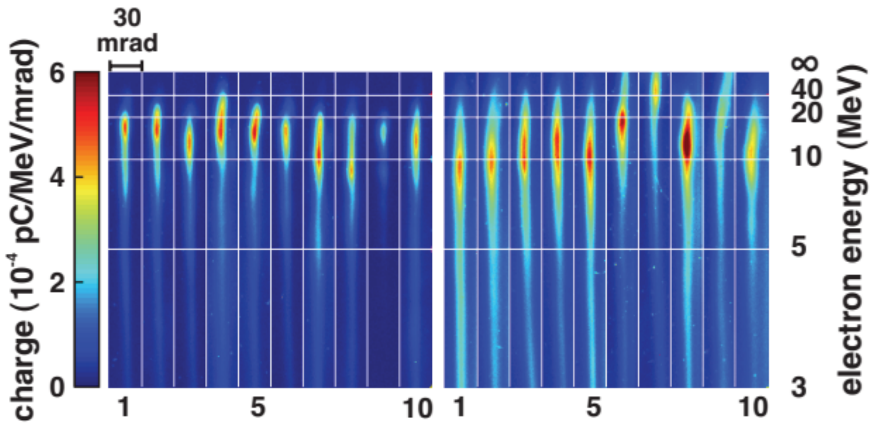

Case I
3.7 TW, 400 psi
Δθy ~ 4.4 mad
Δθz ~ 9.2 mrad

Case III
3.2 TW, 600 psi
Δθy ~ 5.5 mad
Δθz ~ 7.6 mrad

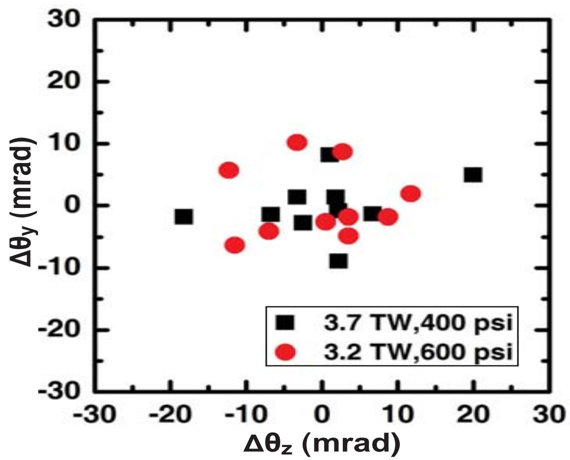

Parameters	3.7 TW, 400 psi	3.2 TW, 600 psi
Peak energy (MeV)	$13.8^{+2}_{-3.3}$	$11.4^{+5.5}_{-1.3}$
Energy spread (FWHM, %)	93^{+77}_{-22}	$199^{+44.5}_{-35.5}$
Charge (>5 MeV, pC)	$11.2^{+3.3}_{-2.9}$	$21.4^{+2.9}_{-3}$

The sub-mm nitrogen jets represents a viable approach for generating tens-of-MeV electrons with satisfactory energy and charge stabilities.

The PIC simulation verifies the free running ionization-induced injection and density down-ramp injection

M.-W. Lin et al., Phys. Plasmas 27, 113102 (2020)

810 nm,
40 fs,
3.2 TW

$a_0 \sim 1.18$ in vacuum

Nitrogen target of 860-μm width

$P_L / P_{cr} \sim 3$

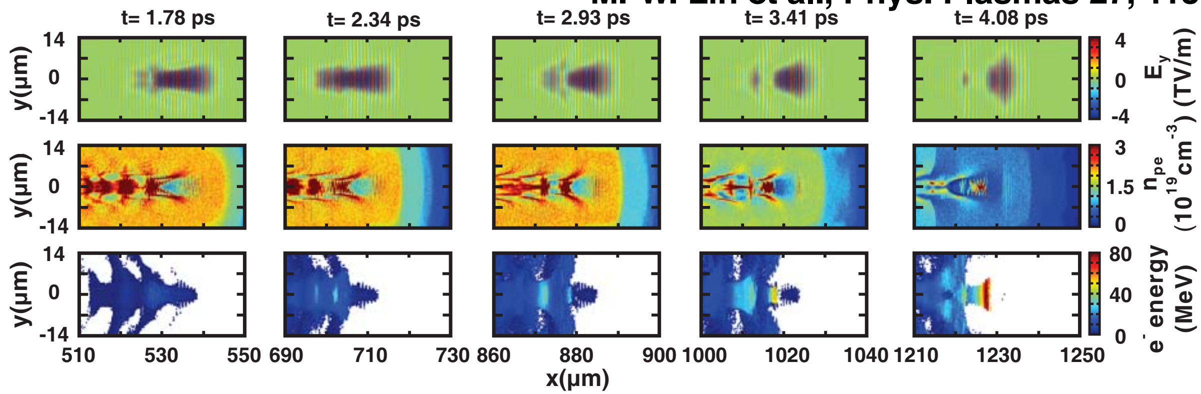

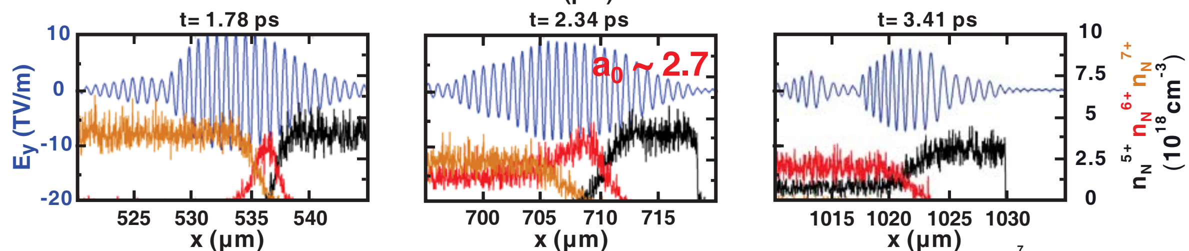

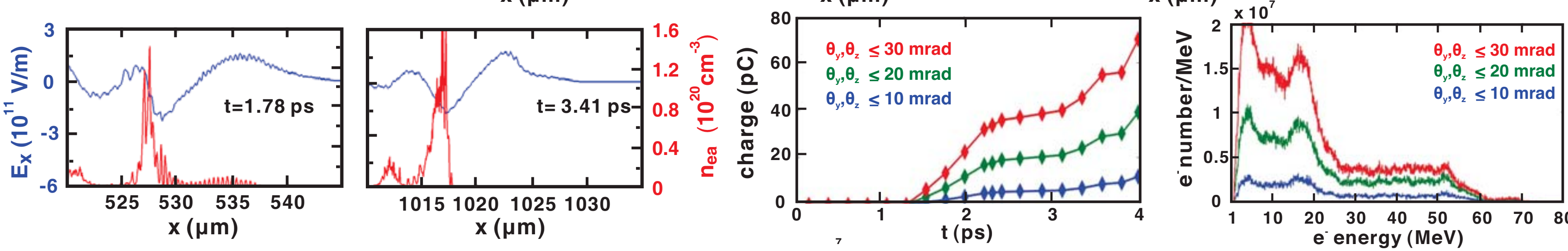

- The peak intensity of the focused pump pulse is greatly enhanced to be $a_0 > 2.5$, enabling the ionization-induced injection with $N^{5+} \rightarrow N^{6+}$ and $N^{6+} \rightarrow N^{7+}$.
- Majority of output electrons are trapped and accelerated during the pulse propagation throughout the rear edge (density down-ramp) of the nitrogen target.

Using orifices of different diameters offers the flexibility for producing nitrogen jets with various density profiles

178-μm orifice, P_L= 1 TW

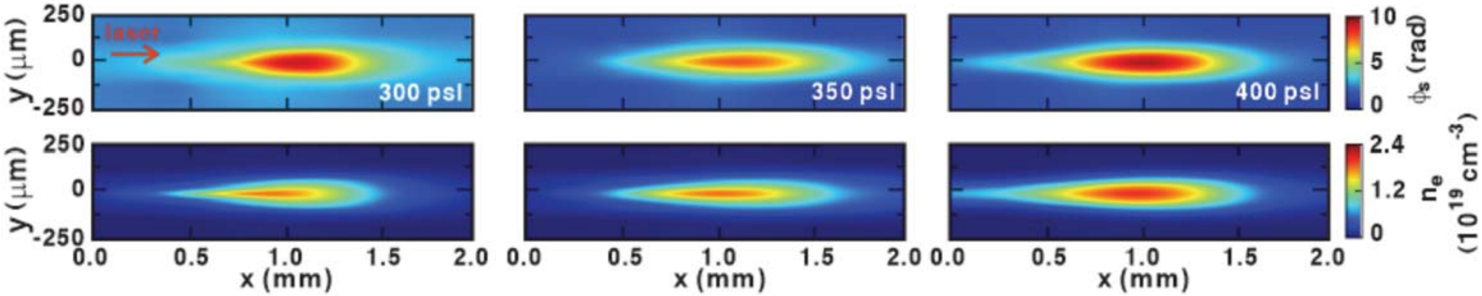

178 μm

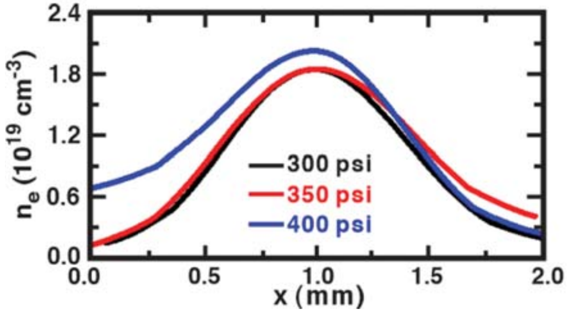

p_N (psi)	178 μm		203 μm	
	n_e (10^{19} cm^{-3})	FWHM (μm)	n_e (10^{19} cm^{-3})	FWHM (μm)
300	1.8	931	1.9	1102
350	1.9	1046	2.1	1206

203 μm

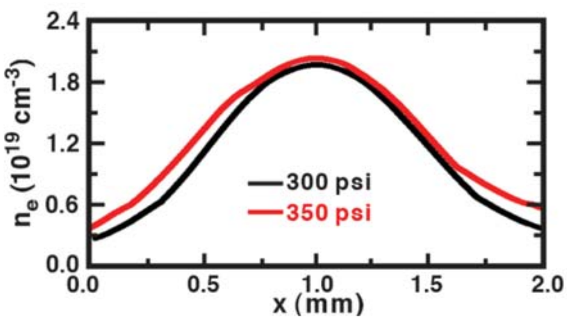

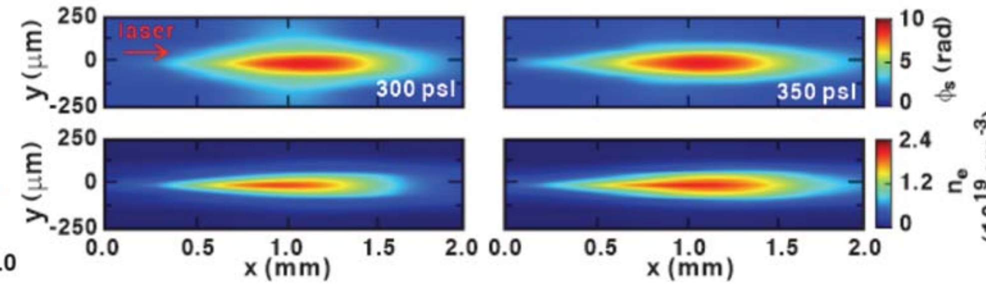

Under same backing pressure, gas jets produced by a 203-μm orifice typically exhibit a higher peak density and a longer target length than those with 178-μm orifice.

Using 1-TW pulse and 178-μm orifice, electron beams can be generated with nitrogen plasmas of a peak density $n_e \sim 2\text{x}10^{19}$ cm^{-3}

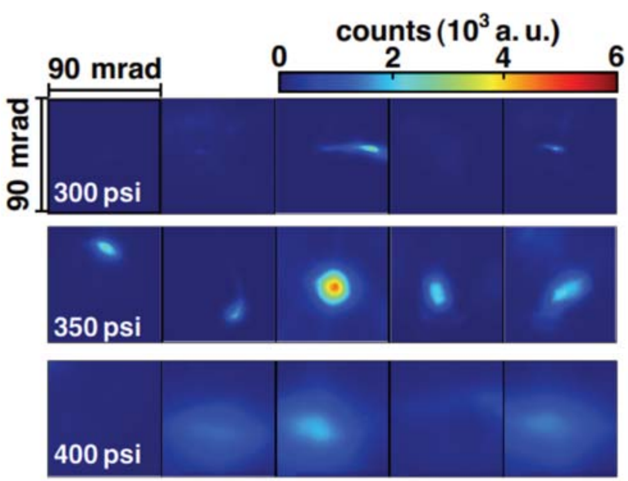

178-μm orifice, P_L= 1 TW

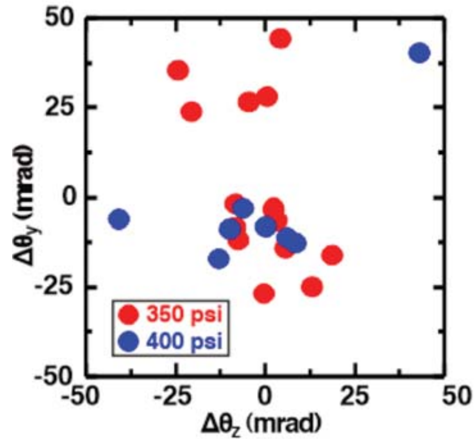

Beam divergence

350 psi	400 psi
$\theta_y \sim$ 20.1 mrad	$\theta_y \sim$ 34.7 mrad
$\theta_z \sim$ 20.7 mrad	$\theta_z \sim$ 54.8 mrad

Pointing fluctuation

350 psi	400 psi
$\Delta\theta_y \sim$ 22.1 mrad	$\Delta\theta_y \sim$ 20.1 mrad
$\Delta\theta_z \sim$ 11.2 mrad	$\Delta\theta_z \sim$ 27.4 mrad

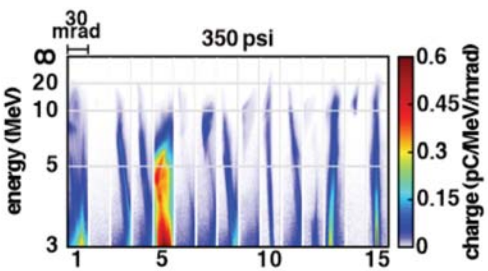

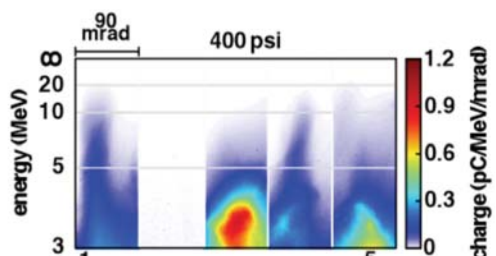

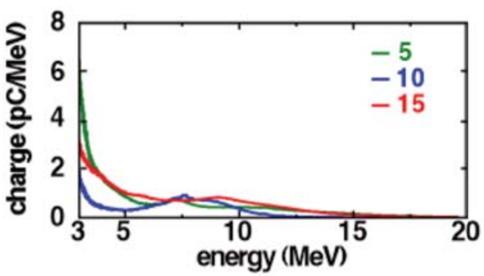

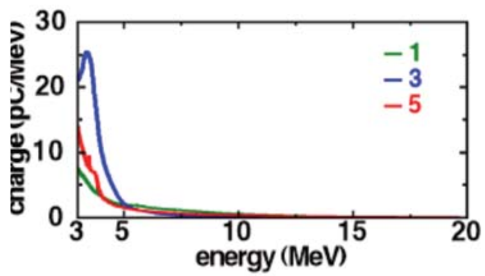

Increasing p_N from 350 psi to 400 psi causes a significant increase of beam divergence and a greater charge for the output electrons.

p_N (psi)	E_P (MeV)	E_{FWHM} (MeV)	Q (> 3 MeV) (pC)
350	$6.2^{+5.7}_{-3.7}$	$8.7^{+11.6}_{-5.7}$	$4.9^{+5.6}_{-3.7}$ (30 mrad)
400	$3.9^{+3.9}_{-3.4}$	$3.9^{+4.6}_{-4.7}$	$40.1^{+35.7}_{-32.9}$ (90 mrad)

With 1-TW pulses, a sub-millimeter nitrogen gas cell can also be utilized for implementing LWFA to routinely generate electron beams

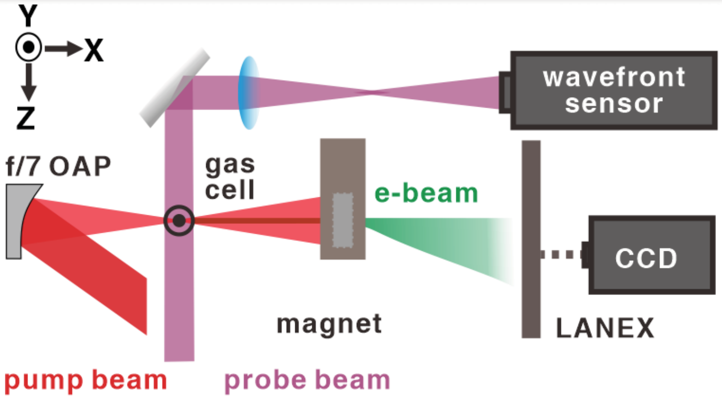

Pump pulse: 40 fs, 810 nm

75% energy (43 mJ) enclosed in a Gaussian-fit profile
Peak intensity I_0 = 1.3x10^{18} W/cm^2 (a_0 = 0.8)

Spot size (FWHM):
vertical ~ 6.5 μm
horizontal ~ 8 μm

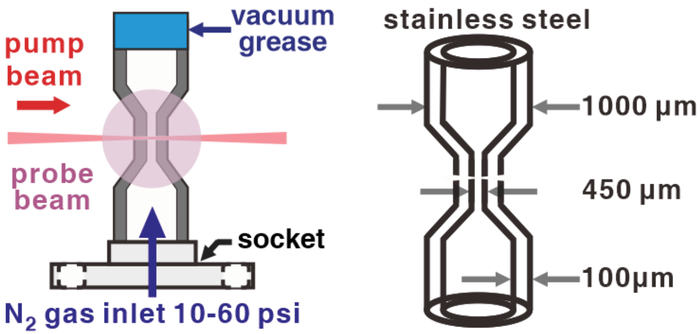

The 450-μm long gas cell was fabricated by shaping a stainless-steel tube with an inner gap of 450 μm between the and then ablating it with 3-mJ pulses to machine the entrance and exit channels.

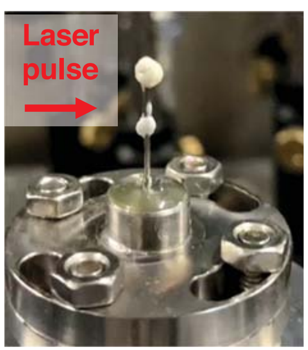

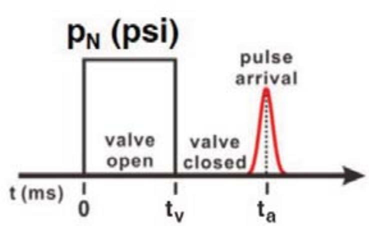

t_v : duration for valve open
t_a : pulse arrival

- Valve opens with t_v = 5 ms.
- Pump pulse entered the cell with t_a = 10 ms.
- The peak density of gas atoms/plasma inside the cell was adjusted by tuning the backing pressure p_N.

A high plasma density $n_e > 3.8 \times 10^{19}$ cm^{-3} is achieved in the cell with a backing pressure of p_N= 20 psi

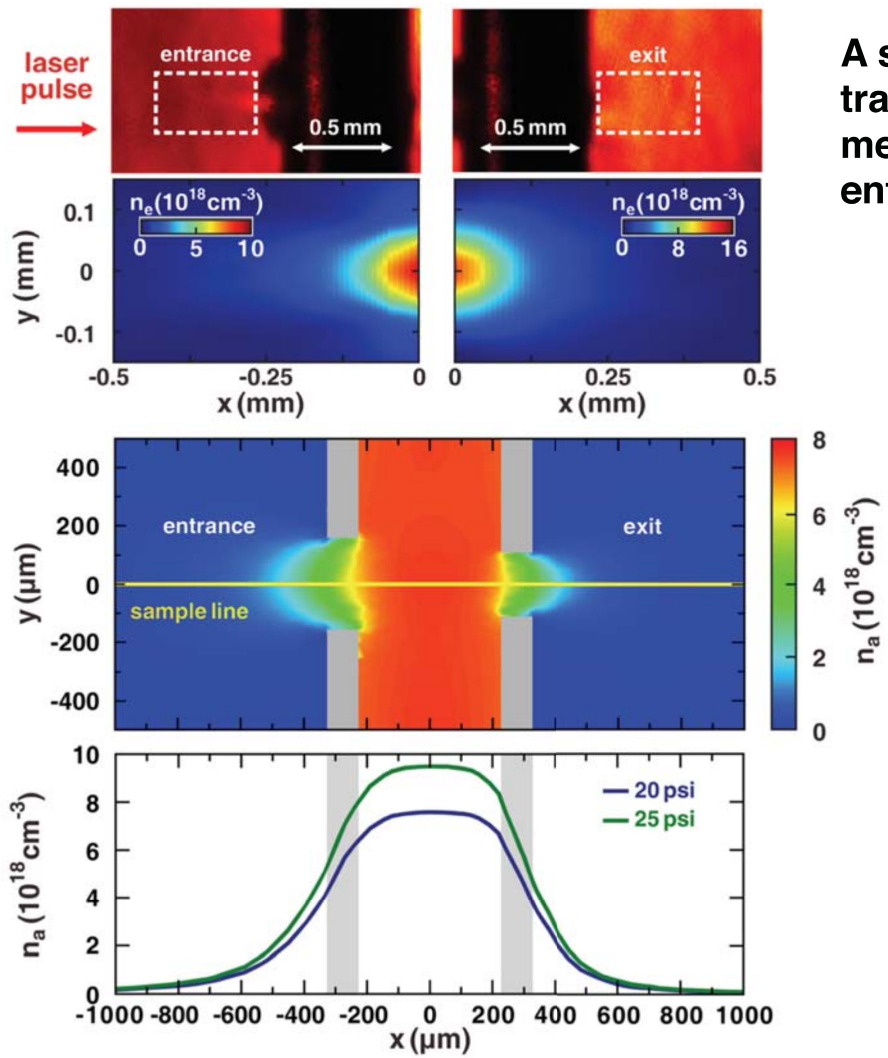

A shadowgraphy probe beam was set to transversely pass through the gas cell and measure the plasma electrons outside the entrance and exit channels.

The distribution of nitrogen atom density (n_a) inside the gas cell was investigated by 3-D computational fluid dynamics (CFD) simulations.

The peak nitrogen atom density (n_a) in the cell :

- **p_N = 20 psi, $n_a = 7.6 \times 10^{18}$ cm^{-3}**
- **p_N = 25 psi, $n_a = 9.5 \times 10^{18}$ cm^{-3}**

As the front foot of the pump pulse ionizes the nitrogen ions to N^{5+}, self-focusing of the pulse is developed with

p_N(psi)	n_e (10^{19} cm^{-3})	P_L/P_{cr}
20	3.8	1.3
25	4.75	1.6

P.-W. Lai et al., Phys. Plasmas 30, 010703 (2023)

With 1-TW pulses, 10-MeV-scale electron beams can be generated routinely at p_N = 20 and 25 psi

P.-W. Lai et al., Phys. Plasmas 30, 010703 (2023)

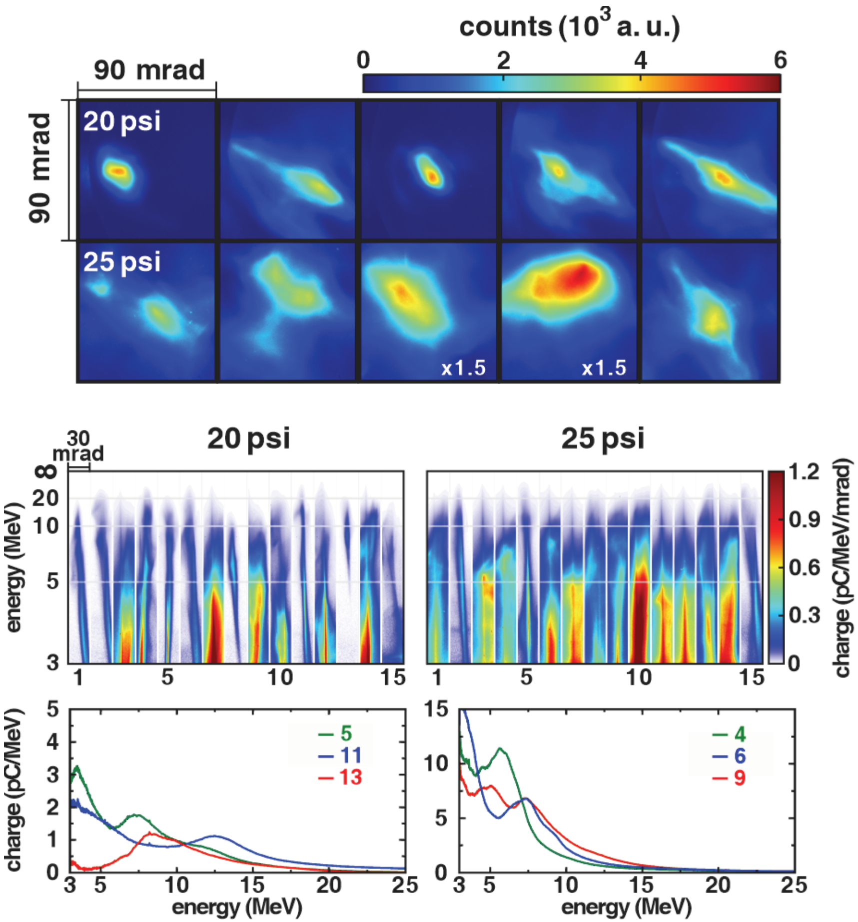

For 15 consecutive shots:

Beam divergence

20 psi	25 psi
θ_y~ 38.3 mrad	θ_y~ 57.5 mrad
θ_z~ 43.4 mrad	θ_z~ 69.9 mrad

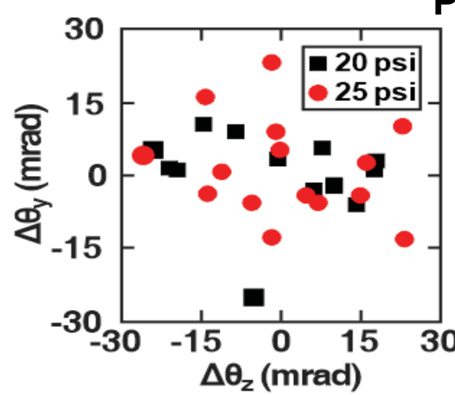

Pointing fluctuation

20 psi

$\Delta\theta_y$~ 8.1 mrad

$\Delta\theta_z$~14.1 mrad

25 psi

$\Delta\theta_y$~10.1 mrad

$\Delta\theta_z$~13.8 mrad

p_N (psi)	E_P (MeV)	E_{FWHM} (MeV)	Q(> 3 MeV) (pC)
20	$8.66^{+3.6}_{-5.5}$	$12.9^{+14.5}_{-5.5}$	$29.14^{+21.1}_{-14.9}$
25	$8.55^{+7.9}_{-2.9}$	$25.69^{+114.5}_{-17.3}$	$61.42^{+25.6}_{-19.1}$

A 25 % increase in nitrogen atom density inside the cell (p_N = 20 psi vs 25 psi) can double the charge but with prominently increased beam divergence.

PIC simulations were performed to examine the self-focusing of the pump pulse and the electron injections in LWFA

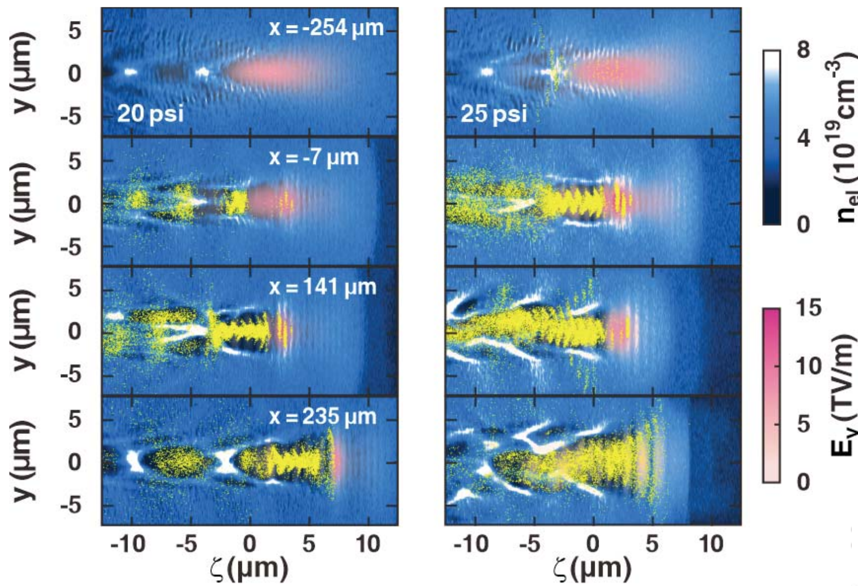

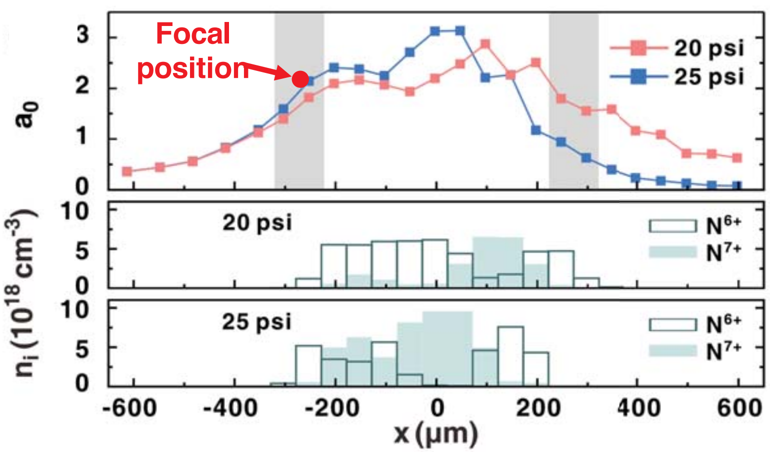

The self-focused pump pulse enables ionization injection from the creation of N^{6+} and N^{7+} when $a_0 > 1.7$.

With p_N = 25 psi, nitrogen ion can be fully ionized to N^{7+} and the pump pulse defocuses considerably because of the overly strong ionization-induced refraction.

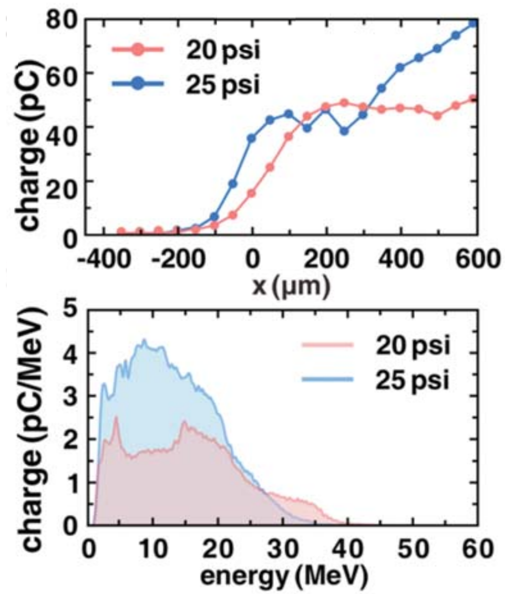

With p_N = 25 psi, it shows the appropriately defocused pump pulse facilitates extra electron injection within the target rear side.

P.-W. Lai et al., Phys. Plasmas 30, 010703 (2023)

Appropriately defocused pump pulse obtained with p_N = 25 psi helps to enhance the down-ramp injection in the target rear side.

P.-W. Lai et al., Phys. Plasmas 30, 010703 (2023)

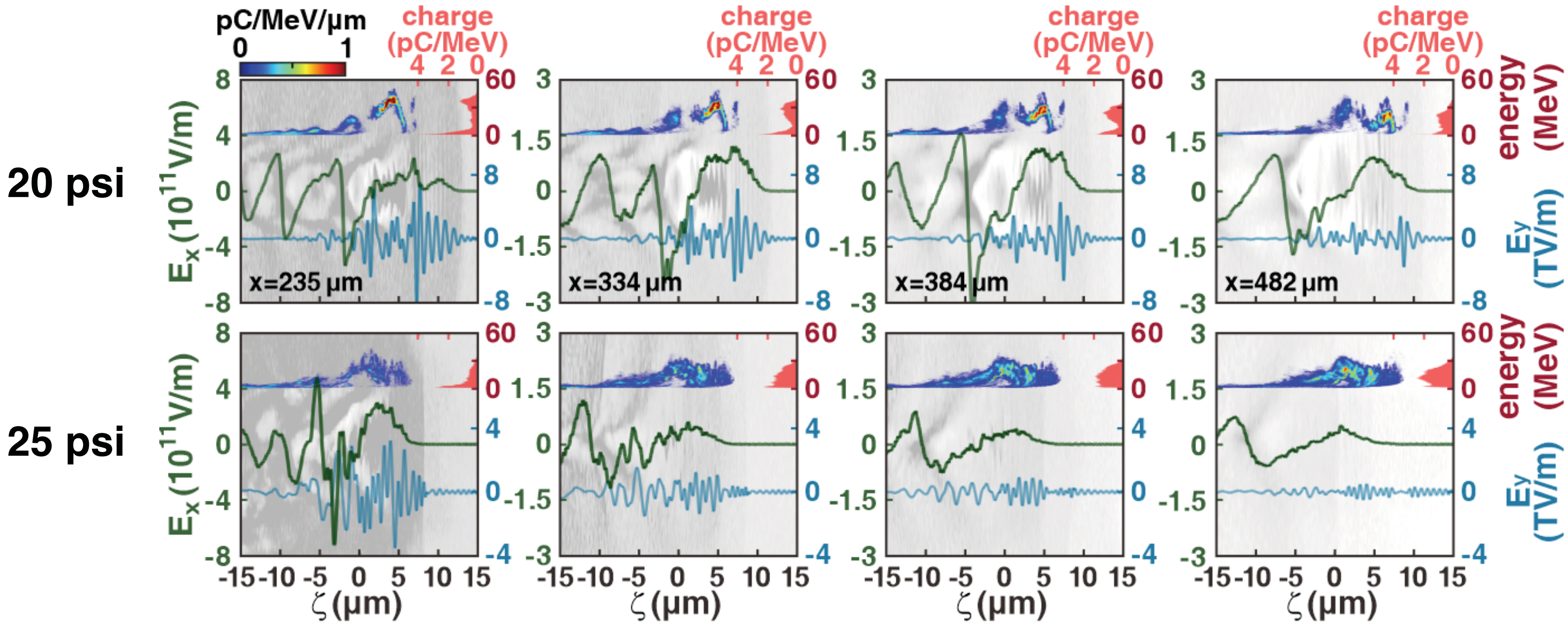

- Significant dephasing is resulted to limit the majority of the accelerated electron to an energy < 20 MeV.
- With p_N = 25 psi, the wakefield Ex degrades into a smoother profile within x ≈ 300–600 *μ*m along with the appropriately defocused pump pulse => Ex overlaps with more electrons in the sheath, so that electron injection becomes more effective to increase the charge of accelerated electrons.

Summary

Our results identify the high potential for implementing sub-mm nitrogen gas jets and gas cells in the future development of high-repetition-rate LWFA driven by few-TW, multi-cycle laser pulses.

- **Compare to gas jets, gas cells can generally work with a low backing pressure < 50 psi to create a sufficiently high gas/plasma density inside its confined space.**
  => use a continuous-flow, low-pressure gas cell in a LWFA system helps to reduce the complexity of sustaining the vacuum level in the accelerator stage.
- **Repetitive irradiation of pump pulses on the cell wall can probably cause rapid heating or even damage to the cell.**
- **One can shape the density profile of gas jets for improving the properties of output electrons but this is challenging in a gas cell.**

This work has been supported by the National Science and Technology Council (NSTC) in Taiwan by Grant No. MOST 110-2112-M-007-027, MOST 111-2112-M-007-033